Non-Linear Effects in Asymmetric Catalysis

Geiger, Yannick; Bellemin-Laponnaz, Stéphane

Published in:
ChemCatChem

DOI:
10.1002/cctc.202200165

Publication date:
2022

ChemCatChem

Research Article
doi.org/10.1002/cctc.202200165

Chemistry Europe
European Chemical Societies Publishing

www.chemcatchem.org

Non-Linear Effects in Asymmetric Catalysis: Impact of Catalyst Precipitation

Yannick Geiger[a, b] and Stéphane Bellemin-Laponnaz*[a]

Non-linear effects between the enantiomeric excesses of both the ligand and the product are ubiquitous phenomena in asymmetric catalysis, allowing asymmetric amplification (or depletion) and are widely used tools for mechanistic investigations. Non-linear effects are caused by catalyst aggregation; however, the effect of catalyst precipitation on NLEs has not been systematically investigated to date, except in special cases such as ternary phase systems. In this article, we show through simulations and with several literature cases at hand how precipitation affects shape and amplitude of NLE curves. The limit of solubility of the homo- or heterochiral dimeric species causes broken-shaped NLE curves or very pronounced NLEs even though the equilibria between the different species in solution are not favorable, at first sight. Peculiar features such as horizontal segments, inverse S-shaped curves and a strong effect of total catalyst concentration are also observed. Overall, this study allows to get a better understanding of chiral catalytic systems and gives an outlook at other types of phase separation leading to NLEs.

Introduction

Asymmetric synthesis is of paramount importance for obtaining enantiopure molecules, in particular in pharmaceutical industry where chiral drugs are almost exclusively applied as single enantiomers.[1] In such catalytic -or stoichiometric- asymmetric syntheses a chiral auxiliary (often a chiral ligand attached to a metal) is used, usually in its enantiomerically pure form in order to maximize the enantiomeric excess of the product (ee_P). However, high ee_P can also be obtained from non-enantiopure compounds if the ligand ee (ee_L) does not scale linearly with ee_P as is usually expected (Figure 1a). Deviations from ee_P vs ee_L-linearity are called non-linear effects (NLE): these can allow high ee_P with a scalemic ligand (even higher than the ligand ee itself) if the NLE is positive (Figure 1b, (+)-NLE); in special cases ee_P may even increase upon ee_L reduction, so that the maximum ee_P is not obtained with the enantiopure but with a non-enantiopure ligand (Figure 1c, *hyperpositive* NLE). In contrast, a negative non-linear effect (Figure 1d, (−)-NLE) leads to a depleted ee_P. NLEs,[2–5] first rationalized by Kagan and coworkers,[6,7] are caused by aggregation of the chiral complexes. This work follows studies on the influence of a compound's enantiomeric purity on its physical properties by Horeau and Guetté[8] and on its chemical reactivity in stoichiometric reactions by Wynberg and Feringa in the mid-70's.[9] It should also be noted that already in 1936 Langenbeck and Triem reported a NLE in the double addition of menthol to oxalyl chloride, along with the conceptual basics for asymmetric amplification and an outlook to catalytic reactions.[10,11]

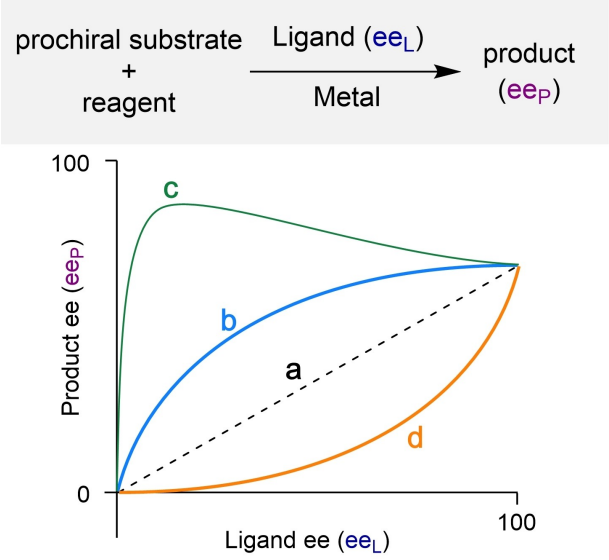

Figure 1. Product ee vs ligand ee-graphs of catalytic asymmetric reactions showing examples for a) no NLE, b) a positive NLE [(+)-NLE)], c) a hyperpositive NLE and d) a negative NLE [(−)-NLE)].

Probing for NLEs has become a tool frequently used for mechanistic investigations in asymmetric catalysis, especially if other analytical tools failed.[12] In addition, the ability of (+)-NLEs to amplify the ee of the chiral source is believed to play a key role in the emergence of biological homochirality and therefore feeds the debate on the origin of life.[13]

To date, models for NLEs consider mostly aggregation levels of 2, as in the Noyori model[14,15] (catalytically active monomers

[a] *Dr. Y. Geiger, Dr. S. Bellemin-Laponnaz*
Institut de Physique et Chimie des Matériaux de Strasbourg
UMR 7504 CNRS-Université de Strasbourg
23 rue du Loess
67000 Strasbourg (France)
E-mail: bellemin@unistra.fr
Homepage: http://www.ipcms.fr
[b] *Dr. Y. Geiger*
Current address: Stratingh Institute for Chemistry
University of Groningen
Nijenborgh 4, 9747 AG (The Netherlands)

Supporting information for this article is available on the WWW under https://doi.org/10.1002/cctc.202200165

in equilibrium with inactive dimers), Kagan's ML_2 model[7] (active dimers and inexistent monomers) and our recent monomer-dimer competition model[16–19] (both monomers and dimers are present and catalytically active). The source of nonlinearity relies in the relative values of the dimerization constants coming into play, which may lead to non-statistical distributions of the different species in solution, as well as in the relative kinetic activities of the different catalysts (except for the Noyori model where only one type of catalyst exists).

Another factor likely to influence that distribution is the selective precipitation of one or several of these aggregates. This is much less discussed, although there are numerous reported experimental cases for catalyst precipitation causing non-linear effects-the first by Narasaka and collaborators[20] in an asymmetric Diels-Alder reaction, followed by many more in transition metal catalysis[16,21–35] and organocatalysis[36–41]-but to date, none of the known models accounts for that possibility. An exception is Kagan's "reservoir effect" model which, however, lacks the mathematical expressions needed to simulate NLE curves properly.[7] More systematic studies were made by Klussmann et al., but with a focus on the special case of ternary phase systems, i.e. simultaneous hetero- and homochiral precipitation, which lead to a horizontal segment in the ee_L vs ee_P-plot ("buffered ee_P").[36–38] Altogether, it was recognized that the interpretation of NLEs could be complicated if catalyst precipitation was not properly taken into account.

Our study aims at filling this gap by expanding previous NLE models to allow for hetero- or homochiral dimer precipitation and thus to study the precipitation's effect on simulated ee_L vs ee_P-curves. We will take some literature cases as a starting point to explore various scenarios and to analyze peculiar features in NLEs (broken-shaped curves, sign switch of an NLE) found both in simulations and in the literature examples. Furthermore, the models allow us to predict other unusual features in NLEs, such as inverse S-shaped curves and horizontal segments. Finally, an outlook concerning other types of phase transition (i.e. liquid-liquid phase separation) will be given.

Results and Discussion

Among the numerous examples of NLEs occurring with precipitation, two stand out through peculiar features: a cyclopropanation reaction reported by Estevan et al.[23] (Figure 2a, black dots) and an alkene hydrogenation reported by Terrade et al. (Figure 2b),[34] both catalyzed by chiral ligand-supported Rh catalysts. The first is remarkable through its broken shape: at more than 80% ligand enantiomeric excess (ee_L) linearity and a homogeneous reaction mixture are observed. Below that value, a (+)-NLE occurs, along with the precipitation of *racemic* catalyst. Such a linear-to-NLE transition was already observed in some homogeneous systems,[2,6,42] however not in the sharp way the data in Figure 2a suggest (which makes them already compatible with existing models, such as Kagan's ML_4 model). In the second example a strong (−)-NLE is observed when catalyst and substrate are added rapidly (Figure 2b, hollow squares), however it changes to a strong (+)-NLE if the catalyst

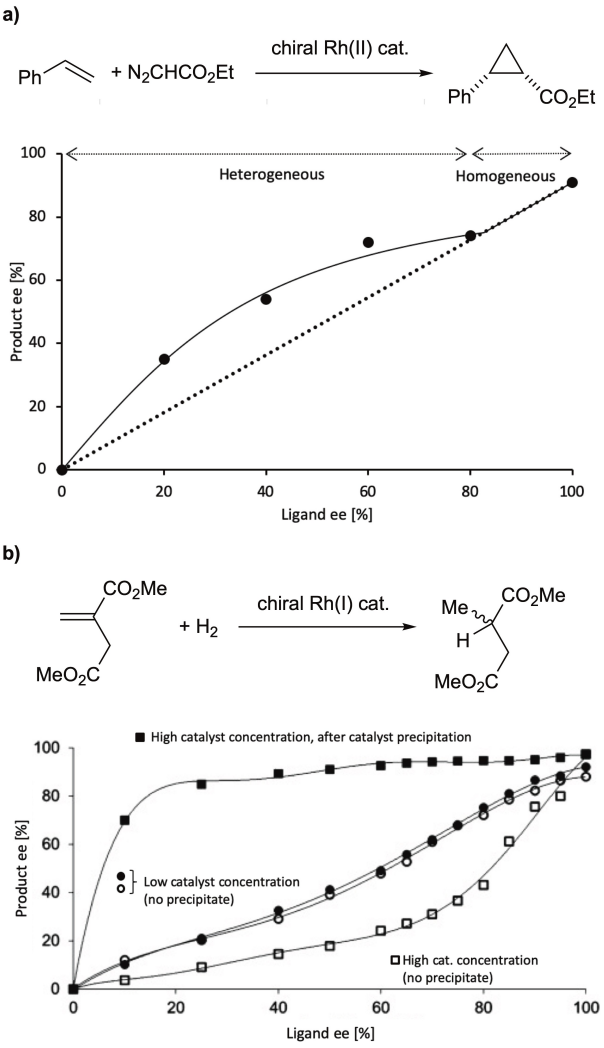

Figure 2. Non-linear effects observed for (a) the enantioselective cyclopropanation of styrene catalyzed by a chiral dirhodium(II) complex (black dots)[23] with a computer-drawn curve calculated from eq. (1–4) (blue line; $k_2 = k_2' = 0$, $ee_1 = 0.91$, $K_{Homo} = 100$, $K_{Hetero} = 195$, $[Cat_{tot}] = 0.004$, $K_s = 1.07 \cdot 10^{-4}$, k_1 and ee_2 not relevant); b) the enantioselective hydrogenation of dimethylitaconate in presence of a chiral Rh(I) complex at 25 mM (squares) or 2 mM (dots) in Rh catalyst, with immediate addition of the substrate (hollow squares/dots) or after a 1 h equilibration time for the catalyst (filled squares/dots), leading to racemate precipitation at 25 mM (filled squares).[34] Graph b) was adapted with permission from reference 34. Copyright Wiley-VCH GmbH.

is let to incubate for 1 h before addition of the substrate, during which a racemic precipitate appears (filled squares; cf. also Klussmann's study on delayed equilibration of proline and TADDOL precipitates).[38] This is a remarkable feature since it allows to study the NLE on one and the same system both with and without catalyst precipitation. Finally, decreasing the concentration in Rh atoms from 25 to 2 mM leads to an almost linear plot, regardless of the protocol used, and to the absence of any precipitate (hollow and filled dots).

Both examples suggest that precipitation of a racemate does not only lead to a (+)-NLE, but can also override the system's inherent tendency to linearity (Figure 2a) or to

asymmetric depletion (Figure 2b). Moreover, Figure 2a shows that precipitation can lead to ee_P vs ee_L-curves with a peculiar, *broken-shaped* aspect. In the following, we will verify whether this can be reproduced in simulations, which account for heterochiral precipitation, by using an extended version of the monomer-dimer competition model we introduced recently.

Model studies: heterochiral dimer precipitation

The *monomer-dimer competition model* is a two-component catalysis where both monomeric and dimeric complexes catalyze the reaction with different enantioselectivities (Figure 3).[16–19] Depending on the parameters chosen it can give rise to classic (+)- or (−)-NLEs, as encountered in the Noyori[14,15] and ML_2[7] models (which can both be considered as special cases within the monomer-dimer competition models), as well as to more exotic ones such as hyperpositive[16] (cf. Figure 1c) or enantiodivergent NLEs,[18] for which we also discovered experimental examples. The overall shape of the NLE curve depends on dimerization constants (K_{Homo} and K_{Hetero}), kinetic constants (k_1, k_2 and k_2'), enantioselectivities (ee_1 and ee_2) as well as on the total catalyst concentration [Cat_{tot}]. All these parameters intervene in equations (1–3) which allow to simulate NLE curves. Here, we introduce an additional solubilization equilibrium for the RS-dimer, whose concentration is now governed by the solubility constant K_S. The mathematical expressions for this model are the same as for the standard model (i.e. all-soluble) one except for β, which becomes a constant depending only on K_{Hetero} and K_S (eq. (4), cf. Supporting Information for the mathematical development). The precipitated $RS_{(s)}$ is not catalytically active and thus influences the overall catalytic outcome by pulling on the various equilibria, as we will show in several computed examples. It is assumed that upon start of the catalytic reaction all equilibria have reached a steady state.

Figure 4 shows simulations following classic scenarios, depicting a Noyori-type[15] (inactive dimers, i.e. $k_2 = k_2' = 0$, Figure 4a) and a ML_2-type[7] system (inactive and inexistent monomers, i.e. $k_1 = 0$ and very high values of K_{Homo} and K_{Hetero}, Figure 4b). The parameters were chosen to generate either a (+)-NLE (Figure 4a) or no NLE at all (Figure 4b). Upon integration of a K_S-value sufficiently low to induce RS-precipitation, the curves become broken-shaped as in Estevan's example: at low ee_L (left part of the graphs) precipitation occurs while at high

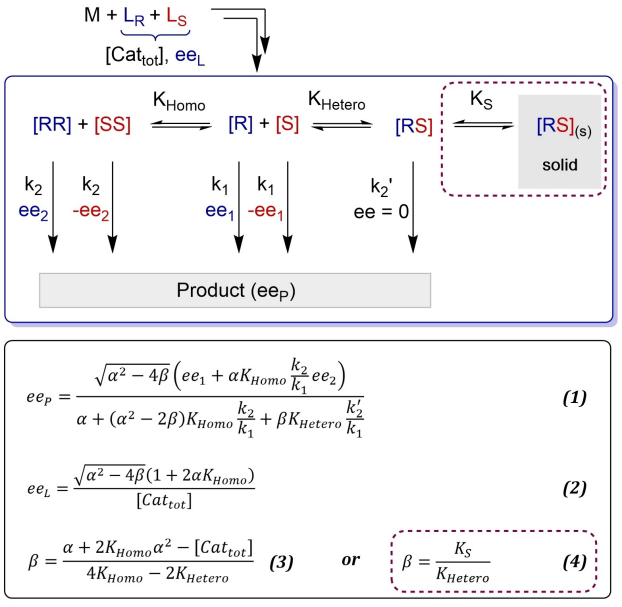

Figure 3. General scheme for the monomer-dimer competition model including a precipitation of the heterochiral dimer RS (with K_S as the solubility constant). The catalytically active species are issued from the irreversible reaction of a metal salt (M) and a chiral ligand (L_R and L_S) with enantiomeric excess ee_L and concentration [Cat_{tot}]. k_1, k_2 and k_2' are rate constants, ee_1 and ee_2 enantioselectivities, K_{Homo} and K_{Hetero} dimerization constants, K_S a solubilization constant, α and β are working variables. The formed chiral product has an overall enantiomeric excess ee_P. Equations (1-3) allow to simulate ee_P vs ee_L-curves following the all-soluble system; eq. (4) replaces eq. (3) if RS-precipitation occurs.

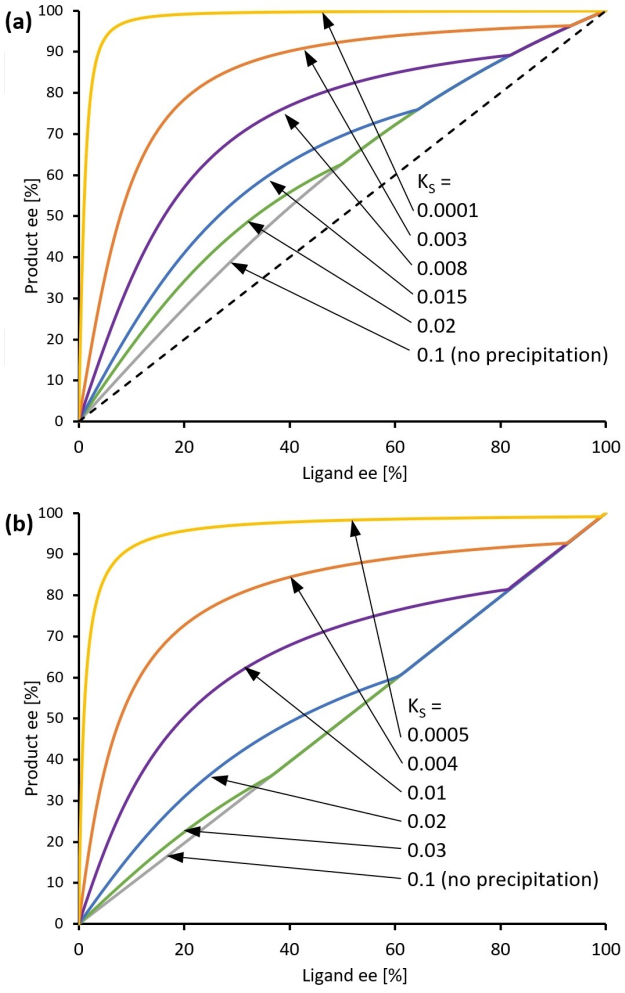

Figure 4. Ee_P vs. ee_L-simulation according to the RS-precipitation model [eq. (1-4)] with K_s as varying parameter. Fixed parameters: (a) $K_{Homo} = 33$, $K_{Hetero} = 150$, $ee_1 = 100\,\%$, [Cat_{tot}] = 0.11 ($k_2 = k_2' = 0$, k_1 and ee_2 not relevant, Noyori-type system), (b) $k_2 = k_2' = 1$, $K_{Homo} = 3.3 \cdot 10^8$, $K_{Hetero} = 1.5 \cdot 10^9$, $ee_2 = 100\,\%$, [Cat_{tot}] = 0.11 ($k_1 = 0$, ee_1 not relevant; the high dimerization constants ensure that monomer concentrations are negligible, as required for a ML_2-type system). The dashed line in a) simulates a linear system based on ee_1 alone.

ee_L (right part) [RS] stays below its solubility limit. The point at which both parts join, the transition point, is defined by [RS] = K_S in the all-soluble model (cf. Supporting information for details). The lower K_S, the more the left part of the broken-shaped curve dominates; at very high K_S the soluble part literally vanishes from the graph. RS-precipitation induces a "local" (+)-NLE which enforces a pre-existing (+)-NLE (Figure 4a) or even induces one in the first place (Figure 4b), which concords nicely with the observations made by Estevan in Figure 2a. Precipitation acts thus in a similar way as an increase of K_{Hetero}[15,18] and allows (+)-NLEs even in special cases where an NLE would be forbidden otherwise (e.g. $k_2' = k_2$ in a ML_2-scenario,[7] as in Figure 4b, or alternatively when $K_{Hetero} = 2K_{Homo}$[15,19]).

Moreover, we could determine a set of parameters that fits well with Estevan's system (continuous line in Figure 2a), reproducing both the linear and the (+)-NLE domains as well as the transition point. The latter can be missed easily if it is far to one side of the graph, or if an insufficient number of datapoints was collected. For example, in the hyperpositive NLE of the NBE-catalyzed addition of $ZnMe_2$ to benzaldehyde, where precipitation occurs at very high ee_L, both all-soluble (with a high K_{Hetero}) and heterochiral precipitation models fit equally well (cf. Supplementary Figure 1).

(+)-NLE induction through racemic precipitation works also with an underlying (−)-NLE, as seen in Figure 5. With a sufficiently low K_S, the precipitation-induced (+)-NLE can completely replace the underlying (−)-NLE; one can thus observe asymmetric amplification despite e.g. $K_{Hetero} < 2K_{Homo}$.[15,18] This concords with Terrade's case in Figure 2b, where the NLE switches from (−) to (+) when the system is given sufficient time to let the racemic catalyst precipitate (although their system is much more complex than our model, with several diastereoisomers present when the system is not left to self-sort).

However, it is worth looking also at intermediate K_S-values (e.g. $K_s = 0.002$ and 0.001, blue and purple highlighted curves): these lead to inverse S-shaped curves with a (+)-NLE on the left and a (−)-NLE on the right part of the graph. So far, S-shaped NLE curves were modelled only with Kagan's ML_4 model, which invokes aggregates as high as tetramers.[7] Here, an aggregation degree of two combined with RS-precipitation is sufficient to induce such a shape. In principle, the transition point between the all-soluble and RS-precipitation regimes makes it visually distinguishable from an ML_4-type S-shaped curve (which is perfectly continuous) but in practice this might not be the case, especially if no or few experimental data points were taken around the transition point.

The second peculiar feature in Terrade's case (Figure 2b) is the switch from a homogeneous system to a system with heterochiral precipitation by increasing the total concentration of catalyst [Cat_{tot}]. This is interesting since [Cat_{tot}] is a parameter easily modifiable for the experimentalist to study NLEs induced by precipitation. Simulations with variation of [Cat_{tot}] in a Noyori-type system (Figure 6) show that within only one order of magnitude of [Cat_{tot}], the catalytic system can be changed from a homogeneous system with linearity to a strong (+)-NLE with RS-precipitation. This concords well with Terrade's case (Figure 2b) where an increase from 2 to 25 mM in Rh catalyst is sufficient to induce a strong NLE.

In addition, scenarios in which both monomers and dimers are present and catalytically active, with opposite enantioselectivities, may be affected by RS-precipitation in a similar way as seen in Figure 4 and Figure 5 (cf. Supplementary Figures 2 and 3 in the Supporting Information): ee_P increases especially at low ee_L, enhancing an already present hyperpositive NLE or turning an inverse (−)-NLE (where catalysis is dominated by the RR dimer, yielding negative ee_P values) into a hyperpositive and

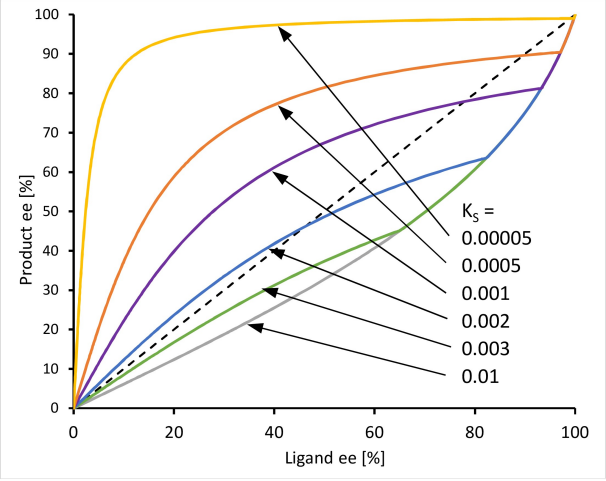

Figure 5. Ee_P vs. ee_L-simulations according to the RS-precipitation model [eq. (1-4)] with K_s as varying parameter. The dashed line simulates a linear system based on ee_1 alone, which intersects the NLE curves (visible on the blue, purple and orange curves) which thus become inverse S-shaped NLEs, with a (+)-NLE at low and a (−)-NLE at high ee_L, Fixed parameters: $K_{Homo} = 150$, $K_{Hetero} = 33$, $ee_1 = 100$, $[Cat_{tot}] = 0.11$ ($k_2 = k_2' = 0$, k_1 and ee_2 not relevant, Noyori-type system).

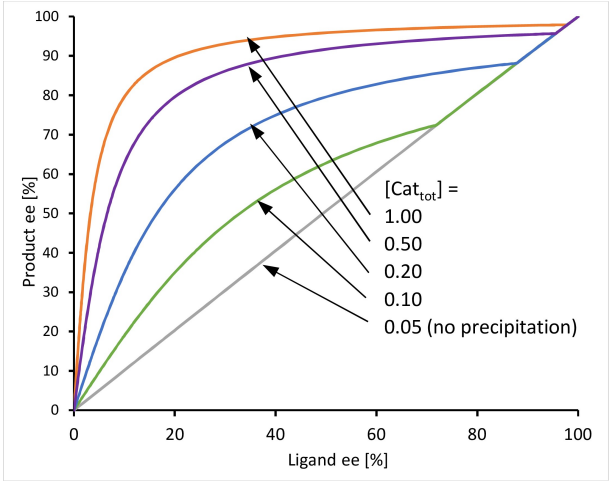

Figure 6. Impact of varying the total catalyst concentration [Cat_{tot}]with heterochiral precipitation (eq. (1–4)). Fixed parameters: $K_S = 0.01$, $K_{Homo} = 120$, $K_{Hetero} = 250$, $ee_1 = 100\%$, $k_2 = k_2' = 0$ (k_1 and ee_2 not relevant), Noyori-type system.

enantiodivergent one. A (−)-NLE can be turned into an inverse S-shaped curve much like in Figure 5 and finally into a hyper-positive NLE.

Further model studies: homochiral dimer precipitation

In a similar way as shown before, one can imagine the precipitation of homochiral instead of heterochiral dimers. Thus, the monomer-dimer competition model can also be extended for homochiral dimer precipitation, by introducing again a solubility constant K_S (Figure 7). Although conglomerate precipitation (i.e. RR and SS dimers crystallize independently of each other, in opposition to racemate crystals where both crystallize within the same lattice in a 1:1 ratio) is less common[43,44] we will also discuss this model as it exhibits interesting properties (cf. Supporting Information for the mathematical treatment and supplementary discussion). The model represents a scenario opposite to the RS-precipitation discussed before: here the racemate remains in solution and the major homochiral dimer enantiomer (in our case RR) precipitates, generating a (−)-NLE at the upper end of the ee_L-scale as shown in simulation graphs (Supplementary Figure 5). It thus acts similar to an increase in K_{Homo} and can induce a (−)-NLE where no NLE (Supplementary Figure 5a) or a (+)-NLE (Supplementary Figure 5b) would be visible otherwise. In the latter case, inverse S-shaped NLEs at intermediate K_S-values are possible, much like those shown for the heterochiral precipitation model in Figure 5. Transition points between RR-precipitation and all-soluble models are also observed. Variation of $[Cat_{tot}]$ (Supplementary Figure 6) has a similar impact as in Figure 6: an increase of an order of magnitude is sufficient to change an all-soluble system with a weak (+)-NLE to a (−)-NLE with homochiral precipitation.

A peculiarity of this model is that it can lead to NLEs with a horizontal segment (i.e. constant product ee when varying ligand ee). This is typically achieved whenever K_S is sufficiently low to also make the minor enantiomer dimer (in our case SS) precipitate, in addition to the major enantiomer (e.g. yellow lines with $K_S = 0.00001$ in Figure 8 and $K_S = 0.001$ in Supplementary Figure 5). ee_P is then equal to 0 between $ee_L = 0$ and the transition point (which here marks the ee_L value where SS has reached saturation); RR precipitates over the whole NLE range and no all-soluble regime is observed. However, RR-precipitation alone can also induce horizontal segments if the RS-dimer is catalytically inactive and highly favored over the homochiral dimers within the monomer-dimer competition model (Figure 8, green and blue lines at $K_S = 0.01$ and 0.001). Under these conditions, as long as RR precipitates, the R and RR complexes in solution are in a constant ratio and the only competent catalysts present, therefore ee_P stays constant over varying ee_L. These features are remarkable since horizontal segments have been observed before only in amino acid-catalysis where simultaneous precipitation of both enantiopure and racemate crystals lead to a "buffered" ee_P.[36,37]

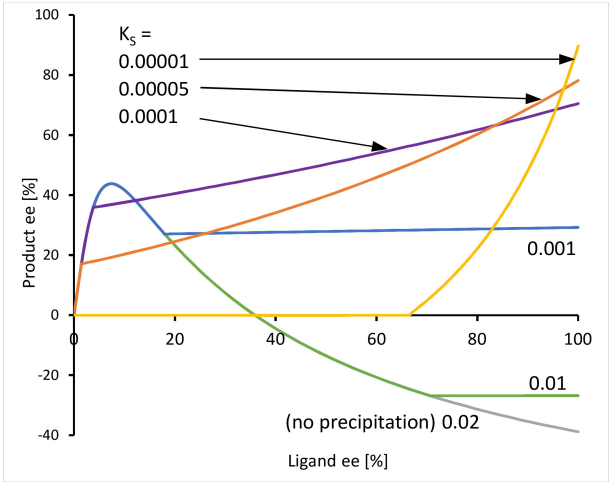

Figure 8. Monomer-dimer competition model with homochiral dimer precipitation. Simulation of the relationship between ee_P and ee_L. Fixed parameters: $k_1 = 10$, $k_2 = 100$, $k_2' = 0$, $K_{Homo} = 3$, $K_{Hetero} = 5000$, $ee_1 = 100\,\%$, $ee_2 = -100\,\%$, $[Cat_{tot}] = 0.11$. The broken shape of the curves originate from a transition between all-soluble (low ee_L) and RR-precipitation (high ee_L), except for the yellow curve ($K_S = 0.00001$) where also the solubility limit of the SS dimer has been reached, leading to RR/SS-coprecipitation instead of an all-soluble regime at low ee_L.

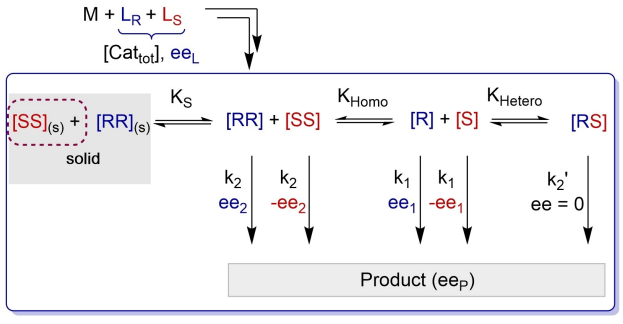

Figure 7. Scheme showing the monomer-dimer competition model with homochiral dimer precipitation. Either only the major enantiomer dimer (here, RR) precipitates with the solubility constant K_S, or both RR and SS precipitate. The equations describing the model and further discussion are found the Supporting Information.

Finally, it should be mentioned that homo- and heterochiral precipitation can occur simultaneously in ternary phase systems. This has already been investigated by Klussmann et al.[36–38] and won't be further developed here.

Outlook: liquid-liquid phase separation

In this context, it is worth looking at another study reported by Šulce and co-workers.[45] Here, amino acid-functionalized platinum nanoparticles (NP) adsorbed on Al_2O_3 catalyze the hydrogenation of ketones. Proline and *tert*-leucine as chiral auxiliaries show no NLE or very weak (+)-NLEs, while phenylglycine gives rise to plots with a linear-to-(+)-NLE transition (Figure 9) similar to Estevan's case in Figure 2a. However, since the system is heterogeneous anyway it is unclear where that transition comes from. A possible explanation is that it originates not from the catalytic process but from the catalyst preparation, which can

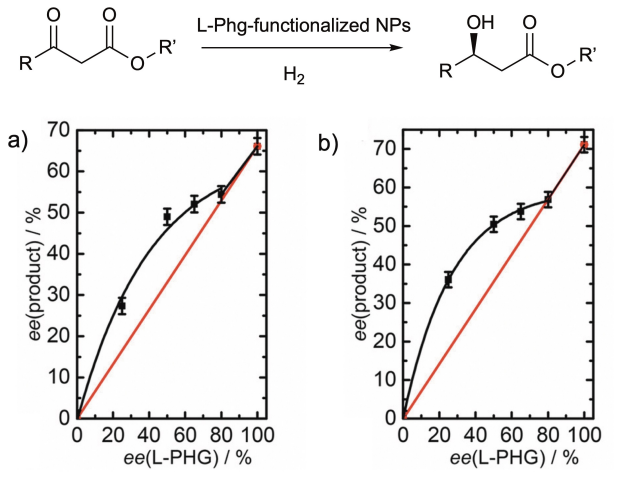

Figure 9. Enantioselective hydrogenation using phenylglycine-functionalized platinum nanoparticles: ee_P vs ee_L-plot with methyl 4,4-dimethyl-3-oxovalerate (R=tBu, R'=Me) as substrate (a) or ethyl 3-oxo-3-phenylpropanoate (R=Ph, R'=Et) as substrate (b). The two figures were reprinted with permission from reference 45. Copyright Wiley-VCH GmbH.

also impact NLEs.[34,46] The amino acid (in excess) is adsorbed onto the Pt NPs in a biphasic cyclohexanone-water mixture. Interestingly, phenylglycine is structurally close to phenylalanine which is prone to liquid-liquid phase separation (i.e. formation of pseudophases in order to shield hydrophobic residues from water)[47,48] and may act as a surfactant in the biphasic mixture, which has also been shown to enable the emergence of NLEs.[49] Thus, one can imagine that stability or reactivity differences between pseudophases (or soft interfaces) of different enantiomeric composition lead to a biased ee of the adsorbed phenylglycine. In principle, one can expect transition points in NLEs to be caused by any type of phase transition, not only solid-liquid. Thus, the transition point seen here might point at a chirally-biased phase separation which would have gone unnoticed otherwise.

Conclusion

This study shows how selective precipitation of dimeric species, either homo- or heterochiral, can generate or influence nonlinear effects in asymmetric catalysis. Catalyst precipitation amplifies existing NLEs or induces NLEs in the first place, even though the underlying thermodynamic equilibria in solution would not allow for a NLE or generate a NLE of opposite sign. This also allows for the emergence of new phenomena such as broken-shaped, partly horizontal or inverse S-shaped NLE curves, which are possible otherwise only with models involving higher-order aggregation. We have identified a transition point, at which the all-soluble model switches into either one of the precipitation models, as a characteristic feature of catalyst precipitation-which in practice may, however, be difficult to spot in certain cases, especially if the experimental curve is not sufficiently resolved around the transition point. Obtaining a large and detailed dataset is good practice and should be done anyway; a change of reaction parameters (catalyst concentration, temperature) does also help by shifting the point into an easier-to-spot part of the NLE curve. Moreover, these observations concord with similar features found in literature examples.

It is interesting to note that reported precipitation-induced NLEs in the literature include only heterochiral precipitation, mostly leading to a (+)-NLE. This highlights the propensity of chiral molecules to form racemate crystals rather than conglomerate crystals.[43,44,50] Beyond precipitation, other phase separations such as liquid-liquid and soft interfaces may also influence NLEs, which then get an increased utility: characteristic features such as a transition point can give a hint for a phase transition coming into play, even if it is invisible to the eye of the experimentalist - as e.g. in liquid-liquid phase separation. This may expand considerably the utility of NLEs as probes for catalytic reaction mechanisms.

Experimental Section

Full description of the models and equations, as well as simulation data, are provided in the supporting information section.

Acknowledgements

We thank Valentin Bellemin-Laponnaz (ISAE-SUPAERO, Toulouse) for helpful discussion in particular with MATLAB software. This work was supported by the Interdisciplinary Thematic Institute ITI-CSC via the IdEx Unistra (ANR-10-IDEX-0002) within the program Investissement d'Avenir.

Conflict of Interest

The authors declare no conflict of interest.

Data Availability Statement

The data that support the findings of this study are available in the supplementary material of this article.

Keywords: asymmetric catalysis · chiral amplification · nonlinear effect

[1] A. N. Collins, G. Shedrake, J. Crosby, *Chirality in Industry II: Developments in the Commercial Manufacture and Applications of Optically Active Compounds*, Wiley, New York, USA, **1992**.
[2] C. Girard, H. B. Kagan, *Angew. Chem. Int. Ed.* **1998**, *37*, 2922–2959; *Angew. Chem.* **1998**, *110*, 3088–3127.
[3] T. Satyanarayana, S. Abraham, H. B. Kagan, *Angew. Chem. Int. Ed.* **2009**, *48*, 456–494; *Angew. Chem.* **2009**, *121*, 464–503.
[4] H. B. Kagan, *Oil Gas Sci. Technol.* **2007**, *62*, 731–738.
[5] H. B. Kagan, *Synlett* **2001**, *2001*, 0888–0899.
[6] C. Puchot, O. Samuel, E. Dunach, S. Zhao, C. Agami, H. B. Kagan, *J. Am. Chem. Soc.* **1986**, *108*, 2353–2357.

[7] D. Guillaneux, S.-H. Zhao, O. Samuel, D. Rainford, H. B. Kagan, *J. Am. Chem. Soc.* **1994**, *116*, 9430–9439.
[8] A. Horeau, J. P. Guetté, *Tetrahedron* **1974**, *30*, 1923–1931.
[9] H. Wynberg, B. Feringa, *Tetrahedron* **1976**, *32*, 2831–2834.
[10] W. Langenbeck, G. Triem, *Z. Phys. Chem.* **1936**, *177 A*, 401–408.
[11] D. Heller, H.-J. Drexler, C. Fischer, H. Buschmann, W. Baumann, B. Heller, *Angew. Chem. Int. Ed.* **2000**, *39*, 495–499; *Angew. Chem.* **2000**, *112*, 505–509.
[12] M. Magrez, J. Wencel-Delord, A. Alexakis, C. Crévisy, M. Mauduit, *Org. Lett.* **2012**, *14*, 3576–3579.
[13] D. G. Blackmond, *Cold Spring Harbor Perspect. Biol.* **2019**, *11*, a032540.
[14] M. Kitamura, S. Okada, S. Suga, R. Noyori, *J. Am. Chem. Soc.* **1989**, *111*, 4028–4036.
[15] M. Kitamura, S. Suga, H. Oka, R. Noyori, *J. Am. Chem. Soc.* **1998**, *120*, 9800–9809.
[16] Y. Geiger, T. Achard, A. Maisse-François, S. Bellemin-Laponnaz, *Nat. Catal.* **2020**, *3*, 422–426.
[17] Y. Geiger, T. Achard, A. Maisse-François, S. Bellemin-Laponnaz, *Chirality* **2020**, *32*, 1250–1256.
[18] Y. Geiger, T. Achard, A. Maisse-François, S. Bellemin-Laponnaz, *Chem. Sci.* **2020**, *11*, 12453–12463.
[19] Y. Geiger, T. Achard, A. Maisse-François, S. Bellemin-Laponnaz, *Eur. J. Org. Chem.* **2021**, *2021*, 2916–2922.
[20] N. Iwasawa, Y. Hayashi, H. Sakurai, K. Narasaka, *Chem. Lett.* **1989**, 1581–1584.
[21] C. Girard, J.-P. Genêt, M. Bulliard, *Eur. J. Org. Chem.* **1999**, *1999*, 2937–2942.
[22] A. Watanabe, K. Matsumoto, Y. Shimada, T. Katsuki, *Tetrahedron Lett.* **2004**, *45*, 6229–6233.
[23] F. Estevan, J. Lloret, M. Sanaú, M. A. Úbeda, *Organometallics* **2006**, *25*, 4977–4984.
[24] F. Caprioli, A. V. R. Madduri, A. J. Minnaard, S. R. Harutyunyan, *Chem. Commun.* **2013**, *49*, 5450–5452.
[25] S. Kanemasa, Y. Oderaotoshi, S. Sakaguchi, H. Yamamoto, J. Tanaka, E. Wada, D. P. Curran, *J. Am. Chem. Soc.* **1998**, *120*, 3074–3088.
[26] D. A. Evans, M. C. Kozlowski, J. A. Murry, C. S. Burgey, K. R. Campos, B. T. Connell, R. J. Staples, *J. Am. Chem. Soc.* **1999**, *121*, 669–685.
[27] C. Bolm, G. Schlingloff, K. Harms, *Chem. Ber.* **1992**, *125*, 1191–1203.
[28] A. Bayer, M. M. Endeshaw, O. R. Gautun, *J. Org. Chem.* **2004**, *69*, 7198–7205.
[29] H. Furuno, T. Hanamoto, Y. Sugimoto, J. Inanaga, *Org. Lett.* **2000**, *2*, 49–52.
[30] T. Satyanarayana, B. Ferber, H. B. Kagan, *Org. Lett.* **2007**, *9*, 251–253.
[31] S. Liu, C. Wolf, *Org. Lett.* **2007**, *9*, 2965–2968.
[32] T. P. Le, S. Tanaka, M. Yoshimura, M. Kitamura, *Bull. Chem. Soc. Jpn.* **2020**, *93*, 1319–1333.
[33] Y. Sekiguchi, N. Yoshikai, *J. Am. Chem. Soc.* **2021**, *143*, 4775–4781.
[34] F. G. Terrade, M. Lutz, J. N. H. Reek, *Chem. Eur. J.* **2013**, *19*, 10458–10462.
[35] T. Nitabaru, A. Nojiri, M. Kobayashi, N. Kumagai, M. Shibasaki, *J. Am. Chem. Soc.* **2009**, *131*, 13860–13869.
[36] M. Klussmann, H. Iwamura, S. P. Mathew, D. H. Wells, U. Pandya, A. Armstrong, D. G. Blackmond, *Nature* **2006**, *441*, 621.
[37] M. Klussmann, A. J. P. White, A. Armstrong, D. G. Blackmond, *Angew. Chem. Int. Ed.* **2006**, *45*, 7985–7989; *Angew. Chem.* **2006**, *118*, 8153–8157.
[38] M. Klussmann, S. P. Mathew, H. Iwamura, D. H. Wells Jr., A. Armstrong, D. G. Blackmond, *Angew. Chem. Int. Ed.* **2006**, *45*, 7989–7992; *Angew. Chem.* **2006**, *118*, 8157–8160.
[39] Y. Hayashi, M. Matsuzawa, J. Yamaguchi, S. Yonehara, Y. Matsumoto, M. Shoji, D. Hashizume, H. Koshino, *Angew. Chem. Int. Ed.* **2006**, *45*, 4593–4597; *Angew. Chem.* **2006**, *118*, 4709–4713.
[40] R. M. Kellogg, *Angew. Chem. Int. Ed.* **2007**, *46*, 494–497; *Angew. Chem.* **2007**, *119*, 498–502.
[41] N. Li, X.-H. Chen, S.-M. Zhou, S.-W. Luo, J. Song, L. Ren, L.-Z. Gong, *Angew. Chem. Int. Ed.* **2010**, *49*, 6378–6381; *Angew. Chem.* **2010**, *122*, 6522–6525.
[42] S. Kobayashi, H. Ishitani, M. Araki, I. Hachiya, *Tetrahedron Lett.* **1994**, *35*, 6325–6328.
[43] T. Buhse, J.-M. Cruz, M. E. Noble-Terán, D. Hochberg, J. M. Ribó, J. Crusats, J.-C. Micheau, *Chem. Rev.* **2021**, *121*, 2147–2229.
[44] J. Jacques, A. Collet, S. H. Wilen, *Enantiomers, Racemates, and Resolutions*, Krieger Publishing Company, Malabar (Florida), **1994**.
[45] A. Šulce, N. Mitschke, V. Azov, S. Kunz, *ChemCatChem* **2019**, *11*, 2732–2742.
[46] T. O. Luukas, D. R. Fenwick, H. B. Kagan, *C. R. Chim.* **2002**, *5*, 487–491.
[47] P. W. J. M. Frederix, R. V. Ulijn, N. T. Hunt, T. Tuttle, *J. Phys. Chem. Lett.* **2011**, *2*, 2380–2384.
[48] Y. Tang, S. Bera, Y. Yao, J. Zeng, Z. Lao, X. Dong, E. Gazit, G. Wei, *bioRxiv* **2021**, DOI 10.1101/2021.04.03.438298.
[49] J. Dutta, N. Wakdikar, S. Tiwari, *Org. Biomol. Chem.* **2017**, *15*, 6746–6752.
[50] C. Dryzun, D. Avnir, *Chem. Commun.* **2012**, *48*, 5874–5876.

Manuscript received: February 1, 2022
Revised manuscript received: February 17, 2022
Accepted manuscript online: February 18, 2022
Version of record online: March 8, 2022